Journal of the Meteorological Society of Japan

EARLY ONLINE RELEASE

This is a PDF preprint of the manuscript that has been peer-reviewed and accepted for publication.

This pre-publication manuscript may be downloaded, distributed, and cited. Since it has not yet been formatted, copyedited, or proofread, there will be a lot of differences between this version and the final published version.

The DOI for this manuscript is

DOI:10.2151/jmsj. 2017-025

J-STAGE Advance published date: August 28, 2017

The final manuscript after publication will replace the preliminary version at the above DOI once it is available.

The Impact of Surface Wind Data Assimilation on the Predictability of Near-Surface Plume Advection in the Case of the Fukushima Nuclear Accident

Tsuyoshi Thomas SEKIYAMA[1], **Mizuo KAJINO, and Masaru KUNII**

Meteorological Research Institute, Tsukuba, Japan

August 4, 2017

---

1) Corresponding author: Tsuyoshi Thomas SEKIYAMA:
Atmospheric Environment and Applied Meteorology Research Department, Meteorological Research Institute, 1-1 Nagamine, Tsukuba, Ibaraki 305-0052 JAPAN.
Email: tsekiyam@mri-jma.go.jp
Tel: +81-29-853-8708
Fax: +81-29-855-7240

Abstract

We investigated the predictability of plume advection in the lower troposphere and the impact of AMeDAS surface wind data assimilation using the radioactive cesium emitted by the Fukushima nuclear accident in March 2011 as an atmospheric tracer. We conducted two experiments of radioactive plume predictions over eastern Japan for March 15, 2011 with a 3-km horizontal resolution using the Japan Meteorological Agency non-hydrostatic weather forecast model and local ensemble transform Kalman filter (JMANHM-LETKF) data assimilation system. The assimilated meteorological data were obtained from the standard archives collected for the JMA operational numerical weather prediction and the AMeDAS surface wind observations. The standard archives do not contain land surface wind observations. The modeled radioactive cesium concentrations were examined for plume arrival times at 40 observatories. The mean error of the plume arrival times for the standard experiment (assimilating only the standard archives) was 82.0 minutes with a 13-hour lead-time on average. In contrast, the mean error of the AMeDAS experiment (assimilating both the standard archives and AMeDAS surface wind observations) was 72.8 minutes, which was 9.2 minutes (11 %) better than that of the standard experiment. This result indicates that the plume prediction has a reasonable accuracy for the environmental emergency response and the prediction can be significantly improved by the surface wind data assimilation.

Keywords: surface wind data assimilation; plume advection predictability; Fukushima nuclear accident; environmental emergency response

1. Introduction

The advection of minor constituents in the troposphere (e.g., water vapor, oxidants, and aerosols) is one of the key processes for numerical weather or environment prediction. Advection, emission, deposition, and chemical/physical changes define the constituent distribution. For weather prediction, the distribution of water vapor influences the coverage and strength of precipitation. Moreover, the distributions of oxidants, aerosols, and their precursors directly impacts human health and indirectly modifies the weather and climate. However, it is difficult to simulate advection in the lower troposphere due to a poor reproducibility of near-surface wind velocities in numerical weather simulations. Numerical weather forecast models cannot explicitly resolve fine-scale structures of real surface wind velocities due to the topographical heterogeneity and the instability (or nonlinearity) of the atmospheric boundary layer (ABL). These sub-grid scale features cause discrepancy between the measured and forecasted variables. Therefore, the observational datasets of surface wind velocities are usually very limited or are avoided for operational weather prediction (e.g., Japan Meteorological Agency (JMA) 2015, in Japanese) to prevent the degradation of initial conditions. To improve near-surface wind prediction, recent studies tried to assimilate surface wind observations over land (e.g., Hacker and Snyder 2005; Benjamin et al. 2010; Hacker and Rostkier-Edelstein 2007; Hacker et al. 2007; Rostkier-Edelstein and Hacker 2010; Ancell et al. 2011, 2015; Ingleby 2015; Bédard et al. 2015, 2017). In these studies, however, the surface wind observations have an influence only on extremely short-term and local forecasts (less than 6 h) even if they have a positive impact. Besides, these past studies have not particularly investigated the

predictability of constituent advection.

In this context, validating constituent advection predictions and understanding the impact of surface wind data assimilation have garnered increasing attention. Especially, the predictability of near-surface plume advection is a crucial factor for the environmental emergency response (EER), in which we have to prepare for the dispersion of hazardous materials emitted from a point source on the ground to the ABL. If the plume prediction has a reasonable accuracy like a weather forecast, people will able to evacuate an area in danger or take shelter in advance (World Meteorological Organization 2006). As mentioned above, the surface wind data assimilation is often very limited or avoided for weather analyses and predictions, although nudging of surface wind observations has been performed for lower tropospheric advection simulations (e.g., the WRF-CMAQ ozone simulation conducted by Li et al. 2016). However, the impact of surface wind data assimilation has not been well investigated for these advection simulations, especially for predictions incorporating high-performance data assimilation.

The investigation of plume advection requires widespread tracer observations with a fine time resolution. Therefore, we used the radioactive cesium emitted by the Fukushima nuclear accident in March 2011 as the atmospheric tracer. The radioactive cesium plume was dispersed from a single source (the Fukushima Daiichi Nuclear Power Plant (FDNPP)); its surface concentration was measured at many locations at a high frequency and with high accuracy (Tsuruta et al. 2014; Oura et al. 2015). This point-source plume is advantageous due to its simple tracer isolation and validation without cross-dispersion. This paper shows the accuracy of the ^{137}Cs plume advection

93 prediction and the impact of surface wind data assimilation on the predictability of the ^{137}Cs plume
94 advection in the following sections.
95
96 **2. Methodology**
97 Generally, atmospheric advection models require a gridded point value (GPV) dataset that
98 contains a meteorological analysis or prediction that is pre-calculated via a high-performance data
99 assimilation system. For example, the JMA operational meso-GPV dataset was used by all regional
100 models that participated in the multimodel intercomparison of Fukushima nuclear pollution
101 predictions (Science Council of Japan (SCJ) 2014) except for two models. One was our model
102 (Sekiyama et al. 2015), which used an original meteorological dataset. The other model used the
103 European Centre for Medium-Range Weather Forecasts (ECMWF) operational global GPV dataset.
104 All models except Sekiyama et al. (2015) utilized the GPV datasets that were prepared by others
105 (i.e., national weather bureaus). However, for the purpose of our investigation, the GPV datasets
106 have to be prepared by our own data assimilation system because we need to arrange a comparison
107 of meteorological analyses performed in the presence or absence of surface wind data assimilation.
108 Hence, we utilized the meteorological data assimilation system of Sekiyama et al. (2015) in this
109 study to prepare the GPV datasets with and without land surface wind data assimilation.
110 The meteorological data assimilation system of Sekiyama et al. (2015) was developed by Kunii
111 (2014) and is composed of JMA's non-hydrostatic regional weather prediction model (JMANHM,
112 cf., Saito et al. 2006, 2007) and the local ensemble transform Kalman filter (LETKF, cf., Miyoshi

and Aranami 2006). This system was driven by 20 ensemble members and a 3-km horizontal resolution within the model domain of eastern Japan (215 × 259 grids, cf., Fig. 2b of Sekiyama et al. 2015) in this study. The covariance localization parameters were set to 50 km in the horizontal, 0.1 natural-logarithm-pressure coordinate in the vertical, and 3 hours in the time dimension for all observations. The boundary conditions for the model domain were provided by the JMA operational global analysis and prediction. Incidentally, JMANHM has been used to produce the JMA operational meso-GPV dataset at a 5-km horizontal resolution since before March 2011 with a four-dimensional variational (4D-Var) data assimilation method; this weather forecast system is called JNoVA (Honda et al. 2005).

Using the abovementioned JMANHM-LETKF data assimilation system, two kinds of meteorological initial conditions were prepared from March 11 to 31, 2011 at 3-hour intervals. One was the standard analysis (STD), which was produced by assimilating only the observations archived for the JMA operational analysis of JNoVA. These observations were collected by land surface observatories (pressure measurements only), satellites (including sea surface wind), radiosondes, pilot balloons, wind profilers, aircrafts, ships, and buoys; the satellite radiances and radar precipitation analyses were excluded in this study. This JNoVA dataset does not contain land surface wind velocity observations.

The other analysis was produced by assimilating the JNoVA dataset and the land surface wind velocity observations collected by AMeDAS. AMeDAS is the acronym of the automated meteorological data acquisition system managed by JMA, which is a land surface observation

network that comprises approximately 1,300 stations throughout Japan with an average interval of 17 km. In this study, we assimilated the land surface wind velocities from more than 200 AMeDAS stations in the model domain (shown in Fig. 1). Fig. 1

For the surface wind data assimilation of the AMeDAS experiment, the height of the surface wind velocity was intended to be fixed at 10 m, because almost every AMeDAS anemometers are installed at 10 m height according to the World Meteorological Organization (WMO) guideline. All observed velocities U_{obs} were transformed into U_{10} using the following formula:

$$U_{10} = \frac{\ln\left(\frac{10}{z_0}\right)}{\ln\left(\frac{z_{obs}}{z_0}\right)} U_{obs}$$

where z_{obs} is the height of the anemometer installation and z_0 is a constant roughness length (1 m); however, the transformation was negligible in the experiment. The observation errors of the AMeDAS surface wind velocity were set to 2 m/s, which is a comparable level to the root mean square errors (RMSEs) of the STD experiment shown in Fig. 2. The RMSEs and correlation coefficients (r) in Fig. 2 were calculated by 1-hour forecasts of the STD and AMeDAS experiments performed every 3 hours from 00:00 UTC on March 11 to 12:00 UTC on March 15, 2011 at the AMeDAS stations used in this study. Fig. 2

Using these meteorological analyses as the initial conditions, two forecast runs (STD and AMeDAS experiments) were performed with the same JMANHM configuration for 48 hours. The boundary conditions were provided by the JMA operational global prediction with the same initial time as JMANHM. The forecast initial time was set to 12:00 UTC on March 14 to reproduce the

151 radioactive cesium plume behavior over the inland area of eastern Japan. According to Nakajima et
152 al. (2017), the radioactive plumes moved primarily over the ocean during the Fukushima nuclear
153 accident in March 2011; however, on March 15–16 and 20–21, the plumes moved deeper inland.
154 However, because there was a widespread precipitation over the Tohoku and Kanto regions on
155 March 20–21, we investigated only the case of March 15–16 in this study. When the precipitation is
156 strong and widespread, the influence of wet deposition on the plume concentration becomes
157 extremely large. The model simulations of precipitation strength and wet deposition are
158 complicated and challenging; therefore, we plan to investigate the March 20–21 event in the future.
159 Plume advection simulations were then driven by the 48-hour meteorological forecast runs using
160 the Eulerian regional air quality model version 2 (RAQM2). RAQM2 was developed by Kajino et al.
161 (2012) and was used for the Fukushima nuclear accident simulation (Adachi et al. 2013; Sekiyama
162 et al. 2015). RAQM2 and JMANHM share the same model domain (eastern Japan) and horizontal
163 resolution (3 km), although the vertical resolution was converted from JMANHM's 60 layers (from
164 the surface to 22 km asl) to RAQM2's 20 layers (from the surface to 10 km asl). All radioactive
165 cesium (^{137}Cs) was expected to be contained in sulfate aerosol particles mixed with organic
166 compounds as shown by Sekiyama et al. (2015).
167 The emission of radioactive cesium was fixed at a constant value (1 Bq/h) because we intended to
168 validate only the plume arrival time at each station to rigorously examine the plume advection
169 predictability. The Fukushima radioactive cesium plume was emitted from the point source; its
170 background concentration was nearly zero before March 2011. The modeled concentration contrast

between the background and the edge of arriving plume was larger than ten orders of magnitude. Therefore, we were easily able to identify the plume arrival time in simulations. We tried many settings of the Fukushima nuclear pollutant simulation using realistic emission rate datasets (e.g., Adachi et al. 2013; SCJ 2014; Sekiyama et al. 2015) and confirmed that we need only relative concentration values if we want to define the edge of radioactive plumes. That is because the background concentration of anthropogenic nuclear products is zero in simulation models, so that the plume edge has a jump of values by more than ten (or sometimes twenty) orders of magnitude. Furthermore, wet deposition in the model was turned off to avoid a plume disappearance caused by the erroneous precipitation in the model.

The modeled plume arrival times were validated by comparing them with the hourly averaged radioactive cesium concentrations measured by Tsuruta et al. (2014) and Oura et al. (2015). Tsuruta et al. (2014) developed a method to retrieve the hourly averaged concentrations of radioactive cesium in the lower atmosphere using suspended particulate matter (SPM) sampling tapes with a detection limit of less than 0.6 Bq/m^3 during the Fukushima nuclear accident. The SPM tapes were collected from the air pollution monitoring network managed by the national government and maintained by prefectural governments. Tsuruta et al. (2014) and Oura et al. (2015) reported the concentration data at 99 SPM tape sampling stations; however, we screened these stations to clearly detect the radioactive plume arrival, which is discussed in the next section. Consequently, the data from 40 stations of the 99 stations were used in this study, as shown in Fig. 3.

Fig. 3

3. Results and Discussion

The plume arrival times at the SPM tape sampling stations were determined with a threshold of 1 Bq/m^3 for the observations and 1×10^{-15} Bq/m^3 for the model experiments. Generally, when the plume arrived, the concentration rose sharply because the background was nearly zero (e.g., Fig. 4a). The observed concentrations changed rapidly from less than the detection limit (approximately 0.6 Bq/m^3) to more than 1 Bq/m^3. The modeled concentrations increased by more than 10 orders of magnitude; the highest modeled concentrations at the SPM tape sampling stations were on the order of $10^{-13} \sim 10^{-11}$ Bq/m^3. Hence, the threshold for the modeled plumes was set to 1×10^{-15} Bq/m^3. For example, the observed plume arrival time and the STD forecasted plume arrival time are shown in Fig. 4a at Station #49 in Kuki City, Saitama Prefecture, based on Oura et al. (2015).

Fig. 4

When a concentration surge was not clearly observed, e.g., Fig. 4b (Station #59 in Chiba City), the arrival time data were not used. In addition, more than one increase in concentration over a short period of time was also observed in a few cases, e.g., Fig. 4c (Station #81 in Ota Ward, Tokyo). In this case, the edge of the observed plume could not be clearly identified and compared with modeled plumes; thus, we omitted these data from the statistical calculations. After the screening, 40 out of the 99 stations of Oura et al. (2015) remained, as shown in Fig. 3. Fortunately, most of the 40 stations were located inland; therefore, it was expected that we could distinctly observe the influence of land surface wind observations on the plume simulation.

The STD experiment did not assimilate the land surface wind observations; namely, it assimilated the observation dataset regularly used in the operational JNoVA system, except for the satellite

211 radiance and radar precipitation data. We have confirmed that the difference between the STD
212 experiment analysis and the operational JNoVA analysis is small. The influence of the satellite
213 radiance and radar precipitation data was negligible for surface wind predictability in this study.
214 The averaged difference (mean error) in the plume arrival times at the 40 SPM tape sampling
215 stations between the observational data and the STD experiment was 82.0 minutes (Table 1); here, Tab. 1
216 the average forecast length was 13 hours. As indicated by the standard deviation (83.4 minutes)
217 compared to this average, the forecasted plume arrival time was often very close to the observations,
218 although there were a few instances of errors exceeding 3 hours. This is thought to represent the
219 realistic ability of state-of-the-art operational weather forecast models and data-assimilation systems
220 to predict plume advection for emergency evacuations.
221 On the other hand, the mean error of the AMeDAS experiment was 72.8 minutes, which was 9.2
222 minutes (11 %) smaller than that of the STD experiment, with a statistical significance level of
223 p-value = 0.008 (Table 1). This result indicates that the land surface wind data assimilation
224 significantly improved the predictability of near-surface plume advection even after a half-day
225 forecast. Although the AMeDAS surface wind observations had only a small positive impact on the
226 surface wind reproducibility as shown in Fig. 2, the impact on the plume predictability was large
227 with a high statistical significance. The accuracy of a half-day plume prediction depends on not
228 only the accuracy of 12-hour-forecasted wind velocities in the vicinity of the plume but also very
229 short-term wind velocity forecasts near the emission source. Therefore, there is possibility that the
230 improvement of the plume arrival time predictability is caused by only the improvement of very

231 short-term forecasts near the emission source. However, at least from a viewpoint of advection
232 prediction, the improvement of the plume predictability was surely kept for longer than 6 hours by
233 the AMeDAS surface wind data assimilation. Besides, the 72.8-minute error will be acceptable for
234 the EER evacuation if the prediction is available with a half-day lead-time.
235
236 **4. Summary**
237 The assimilation of AMeDAS surface wind data has a positive impact on the predictability of
238 plume advection in the lower troposphere, at least in cases of wintertime air pollution over complex
239 terrain, e.g., the Fukushima nuclear accident. The plume arrival prediction has a 72.8-minute error
240 with a half-day lead-time at Tohoku and Kanto regions for March 15, 2011 using the AMeDAS
241 surface wind data assimilation. If the plume arrival prediction was obtained for the EER with an
242 accuracy of the AMeDAS experiment in this study, the information could be used for the
243 evacuation or sheltering. Furthermore, a similar strategy for improving advection predictability
244 would be applicable to near-surface water vapor, oxidant, and aerosol predictions by using surface
245 wind data assimilation.
246
247 **Acknowledgments**
248 We thank Dr. Tsuruta and his colleagues for providing us with their SPM tape radioactive cesium
249 data. The JMA headquarters provided the weather analysis, prediction, JNoVA, and AMeDAS
250 datasets used in this study. This work was supported by JSPS KAKENHI Grant Number

JP24340115, JP16H02946, JP16H04051, JP26800247, JP17K00533, MEXT KAKENHI Grant Number JP24110003, and the Japan-France Integrated Action Program (SAKURA) of JSPS/MAEDI.

References

Adachi, K., M. Kajino, Y. Zaizen, Y. Igarashi, 2013: Emission of spherical cesium-bearing particles from an early stage of the Fukushima nuclear accident, *Sci. Rep.*, **3**, 2554, doi:10.1038/srep02554.

Ancell, B. C., C. F. Mass, and G. J. Hakim, 2011: Evaluation of surface analyses and forecasts with a multiscale ensemble Kalman filter in regions of complex terrain, *Mon. Wea. Rev.*, **139**, 2008–2024, doi:10.1175/2010MWR3612.1.

Ancell, B. C., E. Kashawlic, and J. Schroeder, 2015: Evaluation of wind forecasts and observation impacts from variational and ensemble data assimilation for wind energy applications, *Mon. Wea. Rev.*, **143**, 3230–3245, doi:10.1175/MWR-D-15-0001.1.

Benjamin, S. G., B.D. Jamison, W. R. Moninger, S. R. Sahm, B. Schwartz, and T. W. Schlatter, 2010: Relative short-range forecast impact from aircraft, profiler, radiosonde, VAD, GPS-PW, METAR, and mesonet observations via the RUC hourly assimilation cycle, *Mon. Wea. Rev.*, **138**, 1319–1343, doi:10.1175/2009MWR3097.1.

Bédard, J., S. Laroche, and P. Gauthier, 2015: A geo-statistical observation operator for the

271 assimilation of near-surface wind data, Quart. J. Roy. Meteor. Soc., 141, 2857–2868,
272 doi:10.1002/qj.2569.
273 Bédard, J., S. Laroche, and P. Gauthier, 2017: Near-surface wind observation impact on forecasts:
274 temporal propagation of the analysis increment, *Mon. Wea. Rev.*, **145**, 1549–1564,
275 doi:10.1175/MWR-D-16-0310.1.
276 Hacker, J. P., and C. Snyder, 2005: Ensemble Kalman filter assimilation of fixed screen-height
277 observations in a parameterized PBL, *Mon. Wea. Rev.*, **133**, 3260–3275,
278 doi:10.1175/MWR3022.1.
279 Hacker, J. P., and D. Rostkier-Edelstein, 2007: PBL state estimation with surface observations, a
280 column model, and an ensemble filter, *Mon. Wea. Rev.*, **135**, 2958–2972,
281 doi:10.1175/MWR3443.1.
282 Hacker, J. P., J. L. Anderson, and M. Pagowski, 2007: Improved vertical covariance estimates for
283 ensemble-filter assimilation of near-surface observations, *Mon. Wea. Rev.*, **135**, 1021–1036,
284 doi:10.1175/MWR3333.1.
285 Honda, Y., M. Nishijima, K. Koizumi, Y. Ohta, K. Tamiya, T. Kawabata, and T. Tsuyuki, 2005: A
286 pre-operational variational data assimilation system for a non-hydrostatic model at the Japan
287 Meteorological Agency: Formulation and preliminary results. *Quart. J. Roy. Meteor. Soc.*, **131**,
288 3465–3475, doi:10.1256/qj.05.132.
289 Ingleby, B., 2015: Global assimilation of air temperature, humidity, wind and pressure from surface
290 stations, *Quart. J. Roy. Meteor. Soc.*, **141**, 504–517, doi:10.1002/qj.2372.

291 Japan Meteorological Agency (JMA), 2015: Kansoku Data Riyou no Genjou to Kadai, *NPD report*
292 *separate volume*, **61**, Japan Meteorological Agency, pp. 98. (in Japanese)
293 Kajino, M., Y. Inomata, K. Sato, H. Ueda, Z. Han, J. An, G. Katata, M. Deushi, T. Maki, N.
294 Oshima, J. Kurokawa, T. Ohara, A. Takami, and S. Hatakeyama, 2012: Development of the
295 RAQM2 aerosol chemical transport model and predictions of the Northeast Asian aerosol mass,
296 size, chemistry, and mixing type, *Atmos. Chem. Phys.*, **12**, 11833–11856,
297 doi:10.5194/acp-12-11833-2012.
298 Kunii, M., 2014: Mesoscale Data Assimilation for a Local Severe Rainfall Event with the NHM–
299 LETKF System, *Wea. Forecasting*, 29, 1093–1105, doi:10.1175/WAF-D-13-00032.1.
300 Li, X., Y. Choi, B. Czader, A. Roy, H. Kim, B. Lefer, and S. Pan, 2016: The impact of observation
301 nudging on simulated meteorology and ozone concentrations during DISCOVER-AQ 2013 Texas
302 campaign, *Atmos. Chem. Phys.*, **16**, 3127–3144, doi:10.5194/acp-16-3127-2016.
303 Miyoshi, T. and K. Aranami, 2006: Applying a four-dimensional local ensemble transform Kalman
304 filter (4D-LETKF) to the JMA nonhydrostatic model (NHM), *SOLA*, **2**, 128–131,
305 doi:10.2151/sola.2006-033.
306 Nakajima. T., S. Misawa, Y. Morino, H. Tsuruta, D. Goto, J. Uchida, T. Takemura, T. Ohara, Y.
307 Oura, M. Ebihara, and M. Satoh, 2017: Model depiction of the atmospheric flows of radioactive
308 cesium emitted from the Fukushima Daiichi Nuclear Power Station accident, *Prog. Earth Planet.*
309 *Sci.*, **4:2**, doi:10.1186/s40645-017-0117-x.
310 Oura, Y., M. Ebihara, H. Tsuruta, T. Nakajima. T. Ohara, M. Ishimoto, H. Sawahata, Y. Katsumura,

311 and W. Nitta, 2015: A Database of Hourly Atmospheric Concentrations of Radiocesium (134Cs
312 and 137Cs) in Suspended Particulate Matter Collected in March 2011 at 99 Air Pollution
313 Monitoring Stations in Eastern Japan, *J. Nucl. Radiochem. Sci.*, **15**, 15–26,
314 doi:10.14494/jnrs.15.2_1.
315 Rostkier-Edelstein, D., and J. P. Hacker, 2010: The roles of surface-observation ensemble
316 assimilation and model complexity for nowcasting of PBL profiles: A factor separation analysis,
317 *Wea. Forecasting*, **25**, 1670–1690, doi:10.1175/2010WAF2222435.1.
318 Saito, K., T. Fujita, Y. Yamada, J. Ishida, Y. Kumagai, K. Aranami, S. Ohmori, R. Nagasawa, S.
319 Kumagai, C. Muroi, T. Kato, H. Eito, and Y. Yamazaki, 2006: The operational JMA
320 nonhydrostatic mesoscale model. *Mon. Wea. Rev.*, **134**, 1266–1298, doi:10.1175/MWR3120.1.
321 Saito, K., J. Ishida, K. Aranami, T. Hara, T. Segawa, M. Narita, and Y. Honda, 2007:
322 Nonhydrostatic atmospheric models operational development at JMA. *J. Meteor. Soc. Japan*,
323 **85B**, 271–304, doi:10.2151/jmsj.85B.271.
324 Science Council of Japan (SCJ), 2014: A review of the model comparison of transportation and
325 deposition of radioactive materials released to the environment as a result of the Tokyo Electric
326 Power Company's Fukushima Daiichi Nuclear Power Plant accident, *Report of Committee on*
327 *Comprehensive Synthetic Engineering*, Science Council of Japan,
328 http://www.jpgu.org/scj/report/20140902scj_report_e.pdf
329 Sekiyama, T. T., M. Kunii, K. Kajino, and T. Shimbori, 2015: Horizontal Resolution Dependence
330 of Atmospheric Simulations of the Fukushima Nuclear Accident Using 15-km, 3-km, and 500-m

331 Grid Models, *J. Meteor. Soc. Japan*, **93**, 49–64, doi:10.2151/jmsj.2015-002.

332 Tsuruta, H., Oura, Y., Ebihara, M., Ohara, T., and Nakajima, T., 2014: First retrieval of hourly
333 atmospheric radionuclides just after the Fukushima accident by analyzing filter-tapes of
334 operational air pollution monitoring stations, *Sci. Rep.*, **4**, 6717, doi:10.1038/srep06717.

335 World Meteorological Organization, 2006: Environmental emergency response: WMO activities,
336 *WMO Bulletin*, **55 (1)**, 37–41.

337

338 List of Figures

339

340 Fig. 1 Locations of the AMeDAS surface wind observing stations used for the AMeDAS
341 experiment from 00:00 UTC on March 11 to 12:00 UTC on March 14, 2011. The letter "P"
342 indicates the location of the Fukushima Daiichi Nuclear Power Plant.

343

344 Fig. 2 Scatter diagrams with RMSEs and correlation coefficients (*r*) between the AMeDAS
345 surface wind observations used in this study and 1-hour forecasts (U_{10} and V_{10}: zonal and
346 meridional winds at 10 m height) of the STD/AMeDAS experiments. The 1-hour forecasts were
347 performed every 3 hours from 00:00 UTC on March 11 to 12:00 UTC on March 15, 2011.

348

349 Fig. 3 Closed squares indicate the SPM tape "radioactive cesium observing" stations of Oura et al.
350 (2015) used in this study. Open squares indicate the SPM tape stations shown in Oura et al.
351 (2015) but not used in this study. The letter "P" indicates the location of the Fukushima Daiichi
352 Nuclear Power Plant.

353

354 Fig. 4 Examples of time series of the radioactive cesium (^{137}Cs) concentrations derived from the
355 SPM tape sampling observations and two model experiments (STD and AMeDAS) from
356 12:00UTC on March 14 to 12:00UTC on March 15, 2011. The advection of the plumes was
357 examined using the data from (a) Kuki City, Saitama Prefecture, and not using the data from (b)
358 Chiba City, Chiba Prefecture, or (c) Ota Ward, Tokyo.

359

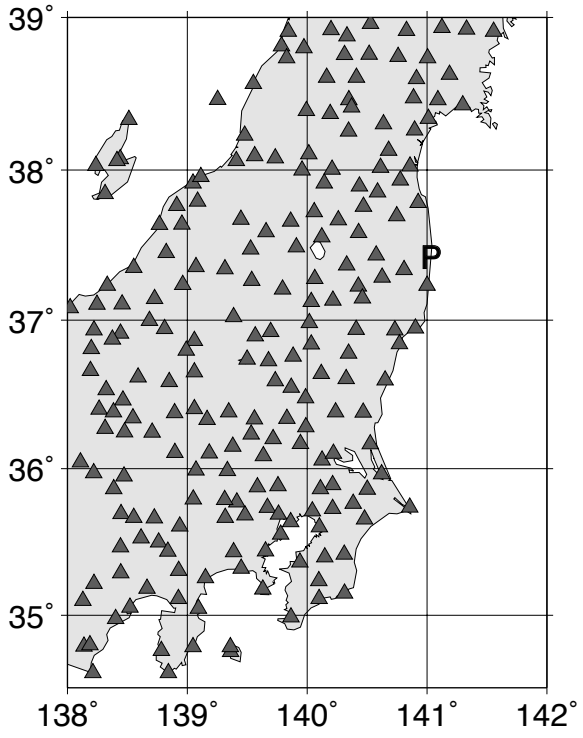

Fig. 1 Locations of the AMeDAS surface wind observing stations used for the AMeDAS experiment from 00:00 UTC on March 11 to 12:00 UTC on March 14, 2011. The letter "P" indicates the location of the Fukushima Daiichi Nuclear Power Plant.

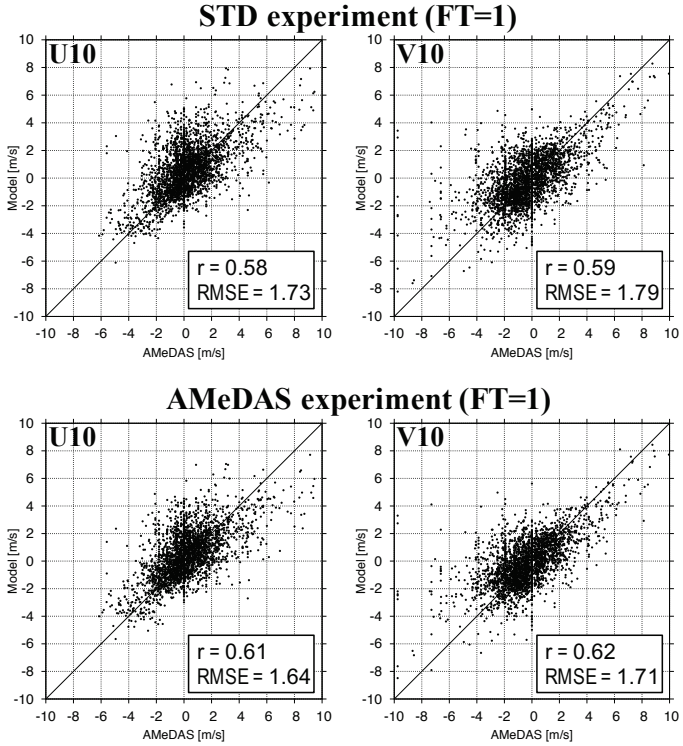

366 Fig. 2 Scatter diagrams with RMSEs and correlation coefficients (*r*) between the AMeDAS
367 surface wind observations used in this study and 1-hour forecasts (U_{10} and V_{10}: zonal and
368 meridional winds at 10 m height) of the STD/AMeDAS experiments. The 1-hour forecasts were
369 performed every 3 hours from 00:00 UTC on March 11 to 12:00 UTC on March 15, 2011.

370

371

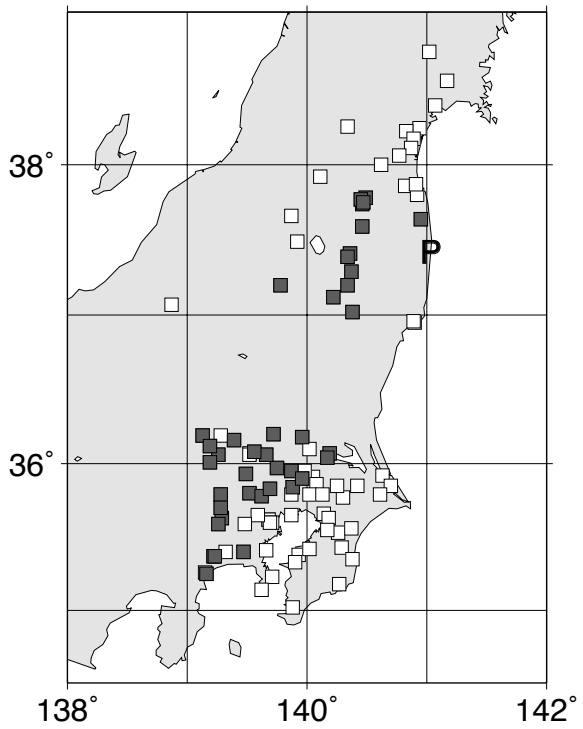

372

373 Fig. 3 Closed squares indicate the SPM tape "radioactive cesium observing" stations of Oura et al.
374 (2015) used in this study. Open squares indicate the SPM tape stations shown in Oura et al.
375 (2015) but not used in this study. The letter "P" indicates the location of the Fukushima Daiichi
376 Nuclear Power Plant.

377

378

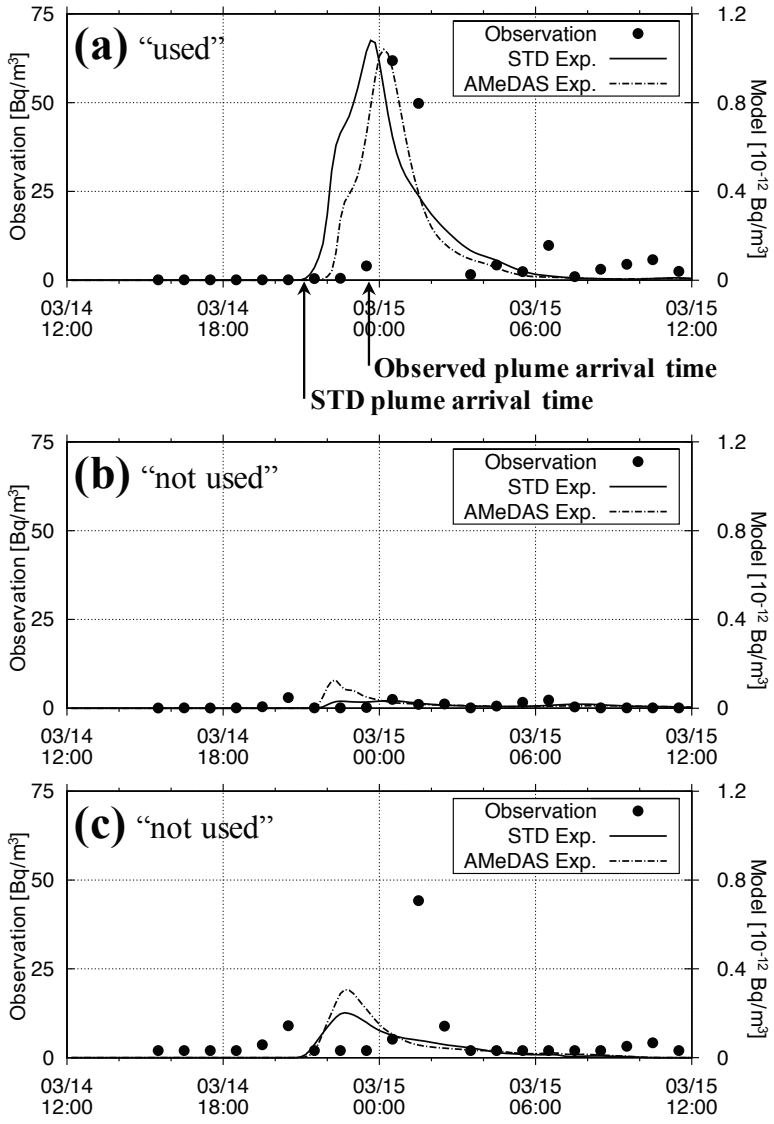

379

380 Fig. 4 Examples of time series of the radioactive cesium (^{137}Cs) concentrations derived from the
381 SPM tape sampling observations and two model experiments (STD and AMeDAS) from
382 12:00UTC on March 14 to 12:00UTC on March 15, 2011. The advection of the plumes was
383 examined using the data from (a) Kuki City, Saitama Prefecture, and not using the data from (b)
384 Chiba City, Chiba Prefecture, or (c) Ota Ward, Tokyo.

385

386

List of Tables

392 Table 1 Mean plume arrival time errors at the 40 SPM-tape sampling stations.

	STD experiment	AMeDAS experiment
mean error (min)	82.0	72.8
standard deviation (min)	83.4	79.6
significance level (p-value)		0.008

393